Asymmetric production of surface-dividing and non-surface-dividing cortical progenitor cells

Takaki Miyata[1,2,3,†], Ayano Kawaguchi[1,*], Kanako Saito[1,2,3], Masako Kawano[1], Tetsuji Muto[1] and Masaharu Ogawa[1,3]

[1]Laboratory for Cell Culture Development, Brain Science Institute, RIKEN, Saitama 351-0198, Japan
[2]Department of Anatomy and Cell Biology, Graduate School of Medicine, Nagoya University, Nagoya 466-8550, Japan
[3]CREST, Japan Science and Technology Corporation (JST), Tokyo 103-0027, Japan
*Present address: Laboratory for Asymmetry, Center for Developmental Biology, RIKEN, Kobe 650-0047, Japan
[†]Author for correspondence (e-mail: tmiyata@med.nagoya-u.ac.jp)

Accepted 16 March 2004

Development 131, 3133-3145
Published by The Company of Biologists 2004
doi:10.1242/dev.01173

Summary

Mature neocortical layers all derive from the cortical plate (CP), a transient zone in the dorsal telencephalon into which young neurons are continuously delivered. To understand cytogenetic and histogenetic events that trigger the emergence of the CP, we have used a slice culture technique. Most divisions at the ventricular surface generated paired cycling daughters (P/P divisions) and the majority of the P/P divisions were asymmetric in daughter cell behavior; they frequently sent one daughter cell to a non-surface (NS) position, the subventricular zone (SVZ), within a single cell-cycle length while keeping the other mitotic daughter for division at the surface. The NS-dividing cells were mostly Hu$^+$ and their daughters were also Hu$^+$, suggesting their commitment to the neuronal lineage and supply of early neurons at a position much closer to their destiny than from the ventricular surface. The release of a cycling daughter cell to SVZ was achieved by collapse of the ventricular process of the cell, followed by its NS division. Neurogenin2 (Ngn2) was immunohistochemically detected in a certain cycling population during G1 phase and was further restricted during G2-M phases to the SVZ-directed population. Its retroviral introduction converted surface divisions to NS divisions. The asymmetric P/P division may therefore contribute to efficient neuron/progenitor segregation required for CP initiation through cell cycle-dependent and lineage-restricted expression of Ngn2.

Supplemental data available online

Key words: Cerebral cortex, Cortical plate, Neuroepithelium, Subventricular zone, Asymmetric cell division, Cell migration, Cell cycle, Cell fate determination, Layer formation, Neurogenin2, Slice culture, Mouse

Introduction

Asymmetric cell division events are important for the generation of cellular diversity in the mammalian cortex. Recent lineage tracing studies have revealed cogeneration of a neuron and a mitotic daughter from a single progenitor cell (N/P division) in the ventricular zone (VZ) of the mid-embryonic cerebral wall (Chenn and McConnell, 1995; Miyata et al., 2001; Noctor et al., 2001) (reviewed by Fishell and Kriegstein, 2003). Although this is amongst the simplest examples of asymmetry in cell output, mechanisms that are thought to be important for generating cellular asymmetry (Knoblich, 2001) might function in broader forms of division, including division that gives rise to two mitotic daughter cells (P/P division) (Qian et al., 1998).

We have recently observed the formation of four-cell clones from single DiI-labeled progenitor cells in retinal slices prepared from embryonic day (E) 17 mice (Saito et al., 2003). Strikingly, the majority of the P/P divisions that formed the retinal four-cell clones were found to be asymmetric, with paired mitotic daughters differing in the trajectory of interkinetic nuclear movement, cell cycle length, and the composition of their daughter cells (i.e. granddaughter cells). Therefore, we sought to determine whether the cerebral wall might also undergo similar asymmetric P/P divisions, focusing on the stage of development just before and during the emergence of the cortical plate (CP) (Fig. 1A). This stage is characterized by a shift in the productivity in the dorsal telencephalon from proliferation without differentiation (‘stage 1’) to differentiation balanced with proliferation (‘stage 2’) (Smart, 1973), as well as a transition from ‘symmetric’ to ‘asymmetric’ divisions in the entire cycling population (Takahashi et al., 1996b). We therefore asked whether the shift in the behavior of the entire population of cells could be explained by possible asymmetric P/P divisions at the single cell level.

For the assessment of asymmetry in a pair of mitotic daughter cells, it is essential to monitor cellular movement prior to division and identify the type of granddaughter cells. Smart (Smart, 1973) confirmed the presence of mitotic figures away from the ventricular surface of the developing cerebral wall, observations originally made in 19th century, and suggested that the earliest formed cells of the CP may originate from non-surface (NS) mitoses. However, the more widely accepted view for the role of the NS-dividing or subventricular

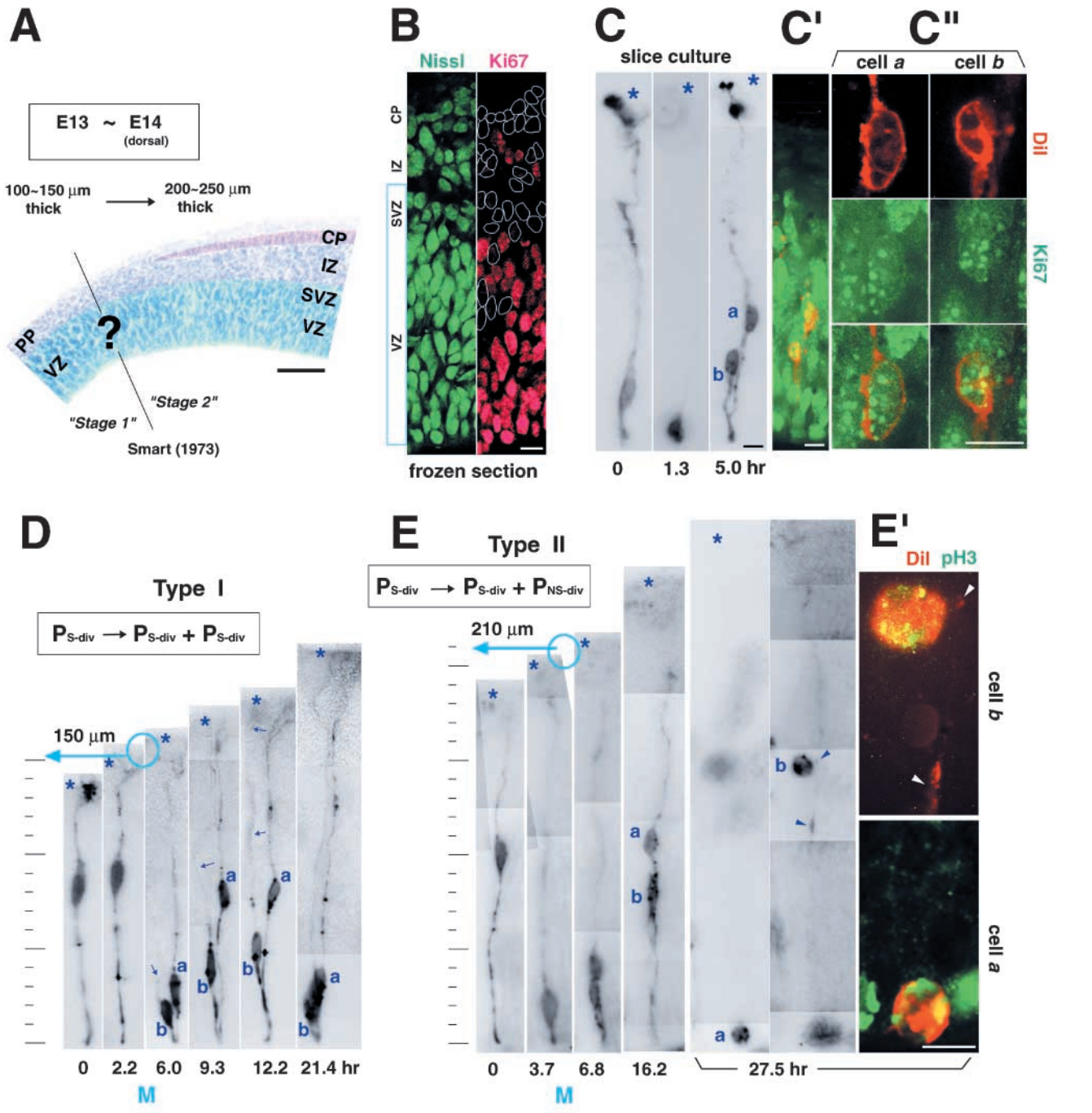

zone (SVZ) progenitor cells in the rodent has been gliogenesis (Altman and Bayer, 1990; Takahashi et al., 1995b). This view has lead to the recent claim that the human neocortical SVZ is evolutionally specialized, that is, massive neuronogenesis occurs in this zone (Letinic et al., 2002). The contribution of NS mitoses to the production of neurons in earlier stages when the preplate is formed was suggested by studies on the cerebral wall of E12-13 rats (Valverde et al., 1995), E10-12 mice (Ishii et al., 2000), and E9-12 mice (Haubensak et al., 2004). Furthermore, the expression of Svet1 was used to link dividing cells in the SVZ of the late embryonic mouse cerebral wall and generation of upper-layer CP neurons (Tarabykin et al., 2001). Just recently, neuron production by NS-dividing cells was most convincingly proved in slice culture of late-embryonic rat cerebral walls (Noctor et al., 2004). These reports suggest that at least some neurons may arise from the NS divisions in the rodent, although the degree of their contribution to the total neuronal output is unclear and should be understood stage by stage.

The origin of the NS-dividing progenitor population is also unclear. Although NS-dividing cells seen in the pallium can arise from the ganglionic eminence (He et al., 2001), the VZ of the pallium is thought to be their primary origin (Altman and Bayer, 1990; Takahashi et al., 1995b). A leading

Fig. 1. P/P divisions predominate during cytogenesis in the pre-cortical plate (CP) stage. (A) Toluidine blue-stained cerebral wall of a B6C3 mouse at E13 depicting the region in question. The present study focuses on cytogenesis in the ventricular zone (VZ) and subventricular zone (SVZ) just before and during the emergence of the CP (pink). Cerebral walls at E14 are also composed of sections in a pre-CP stage, mainly in the dorsal region. Smart (Smart, 1973) suggested that a transition from the proliferation-dominant 'stage 1' to 'stage 2' which balances proliferation and differentiation (see text for detail) occurs in the region that we targeted for the analysis of division patterns. IZ, intermediate zone; PP, preplate. (B) Frozen section of an E14 dorsal region, doubly stained with anti-Ki67 and NeuroTrace (for 'fluorescent Nissl stain'). We counted Ki67-positive and Ki67-negative (outlined) cells in the VZ+SVZ at E13, E14 and E15 to obtain percentage Ki67-positive/Nissl-positive (see Table 1). (C) Slice culture showing a DiI-labeled progenitor that divided at the ventricular surface to give rise to two daughter cells both of which were positive for Ki67 (C′, merged image from photographs using a 40× objective; C″, observation using a 100× objective with optical slice of 1.2 μm). (D) Some forms of P/P division give rise to two daughter cells that divide at the ventricular surface ($P_{S\text{-}div} \rightarrow P_{S\text{-}div}+P_{S\text{-}div}$). Daughter cell 'a' inherited the parent cell's basal process, whereas the cell 'b' extended a new process (arrowed) to the pial surface (asterisk). The trajectory of the interkinetic nuclear movement often differed between such paired surface-dividing (S-div) cells, with quicker and greater ascent by the inheritor of the basal process. (E) Another type of P/P division produces a daughter cell that divides at the surface and another that does not. One of the mitotic daughters born at the surface divided away from the surface (cell 'b'), whereas its sister cell ('b') divided at the surface [entrance into M phase was confirmed by immunostaining with anti-phosphohistoneH3 (pH3), E′] ($P_{S\text{-}div} \rightarrow P_{S\text{-}div}+P_{NS\text{-}div}$). Note that the cell 'b' did not inherit the parent's radial process (arrowhead). The thickness of the cerebral wall when the first mitosis had (or would have) occurred was measured (approximately 150 μm in D; approximately 210 μm in E) to examine the relationship between the frequency of occurrence of each P/P-division pattern and developmental stage (Table 2). Scale bars: 100 μm in A; 10 μm in B,C,C′,C″,E′.

hypothesis predicts that the NS-dividing population arises from the VZ by E13 in mice and by E15 in rats and stays mainly in the SVZ without exhibiting interkinetic nuclear movement and without receiving a further supply of cycling cells from the VZ (Altman and Bayer, 1990; Takahashi et al., 1995b; Nowakowski et al., 2002); this has yet to be rigorously demonstrated. In this study, therefore, we asked whether P/P divisions at the ventricular surface provide these NS-dividing cells. Studying the cellular and molecular mechanisms of normal NS mitoses should also facilitate the analyses of abnormal NS-divisions in mutant animals (Estivill-Torrus et al., 2002; Ferguson et al., 2002).

We used a slice culture system (Miyata et al., 2001; Miyata et al., 2002; Saito et al., 2003) combined with immunohistochemistry and in vivo experiments to monitor progenitor cells in the cerebral wall. We directly observed that P/P divisions were the dominant form of division taking place at the ventricular surface of the cerebral wall around the emergence of the CP. The majority of the P/P divisions supplied one mitotic daughter cell from the ventricular surface to a NS position within a single cell cycle, and the S-to-NS supply of a mitotic daughter was achieved by the loss of a ventricular process by the daughter cell by the end of G2 phase. Also, the NS mitoses were mostly positive for Hu and generated a pair of Hu^+ neuron-like cells. Neurogenin2 (Ngn2), a basic helix-loop-helix-loop (bHLH) transcription factor known to regulate neuronogenesis in the dorsal telencephalon (Sommer et al., 1996; Fode et al., 2000; Nieto et al., 2001) (reviewed by Ross et al., 2003), was detected in a cell cycle-dependent manner, with the highest and broadest expression during G1 phase and a weaker and more NS population-restricted pattern towards M phase. Finally, cells infected with Ngn2 retrovirus showed a significantly higher percentage for NS mitoses compared with those infected with control virus. Accordingly, we propose that commitment to the neuronal lineage, accompanied by the loss of the ventricular process, occurs in a mitotic cell prior to the completion of G2 phase, and the asymmetric P/P division that generates such a NS-dividing mitotic cell, as well as a S-dividing mitotic cell, contributes to the efficient segregation of neurons and cycling cells, a process required in the pre-CP stage.

Materials and methods

Slice culture

Coronal slices were prepared from B6C3 mice at E13 and E14 (plug day=E0), and cultured in collagen gel as previously described (Miyata et al., 2001). Modifications in oxygen concentration (40%, instead of 20%) (Miyata et al., 2002) and DiI-labeling (gentler labeling in culture medium with smaller DiI crystal) (Saito et al., 2003) were effective for extended culture. Time-lapse recording was performed manually as used previously (Miyata et al., 2001; Miyata et al., 2002).

Immunohistochemistry

Cultured slices were fixed in 4% paraformaldehyde for 10 minutes, vibratome-sectioned, treated with antibodies, and subjected to confocal microscopy, as described (Miyata et al., 2001). For in vivo analyses, mice [E13-P0 (P0=day of birth)] were transcardially perfused with PLP fixative (McLean and Nakane, 1974), postfixed in the same fixative for 30-60 minutes on ice, immersed in 20% sucrose, embedded in O.C.T. compound (Miles), and then frozen and coronally sectioned (15 μm). Primary antibodies used: Ki67 (mouse IgG, Novocastra); pH3 (rabbit, UpDate Technology); p-vimentin [mouse IgG (4A4), MBL]; GFP (rat IgG, Nakarai; rabbit, MBL), Hu [mouse IgG (16A11), Molecular Probes]; p27 (mouse IgG, Transduction Laboratories); Ngn2 [rabbit, gift from Masato Nakafuku (Cincinnati Children's Hospital Research Foundation)]; BrdU (mouse IgG, Sigma); Nestin [mouse IgG (Rat401), Hybridoma Bank]; anti-endothelial cell [mouse IgG (#16985), Chemicon]. Some sections were treated with NeuroTrace 500/525 (Molecular Probes) for green fluorescent Nissl staining.

Virus generation and infection

Control-GFP retrovirus, made by inserting IRES-EGFP from pIRES2-EGFP (Clontech) into pLNCX2 (Clontech), and Ngn2/GFP retrovirus, made by inserting ngn2 from pCS2-ngn2 (gift from Jacqueline E. Lee, University of Colorado at Boulder, CO, USA) or pCLIG-ngn2 (gift from Ryoichiro Kageyama, Kyoto University, Japan) vectors into control-GFP, were individually transfected into Ψ2MP34, an ecotropic packaging cell line (Yoshimatsu et al., 1998), using LipofectAMINE (Invitrogen). Supernatant was collected and concentrated, according to Nanmoku et al. (Nanmoku et al., 2003), and injected, through in utero surgery, into lateral ventricles of E12 B6C3 mice. Prior to the retrovirus experiments, we used in utero electroporation (Tabata and Nakajima, 2003) to examine the effect of expression of pCLIG-ngn2 and pCS2-ngn2 on mitosis position, and we found that the total number of NS mitoses [both those expressing a plasmid marker (myc or GFP) as well as those not expressing] was

significantly increased (T. Miyata, unpublished). Because myc$^+$ or GFP$^+$ cells were diffusely found in the VZ at 24 hours after electroporation and all were found to be neurons at 48-72 hours, we considered that Ngn2, through its neuron-inducing activity, may have changed the overall neuroepithelial structure in the VZ, leading to the reporter-negative NS mitoses. To avoid such a technical problem, Ngn2/GFP virus was used at a lower titer (3-10×10^8 cfu/ml) compared with control-GFP (3-4×10^9 cfu/ml). GFP adenovirus, of which GFP expression is driven by the CAG promoter (T. Muto, unpublished), was prepared and injected, by in utero surgery, into the lateral ventricles of E13 B6C3 mice according to previously described methods (Tamamaki et al., 2001; Hashimoto and Mikoshiba, 2004).

Analysis

Region and stage

Immunohistochemical quantifications were performed using coronal sections lying between the anterior margin of the foramen of Monro and the anterior tip of the hippocampal formation proper. Because CP formation (Fig. 1) is initiated rostrolaterally at E13 and proceeds dorsomedially by the end of E14 (Smart, 1973; Smart and McSherry, 1982), we mainly examined dorsolateral and dorsal areas in E13 sections and dorsal and dorsomedial areas in E14 sections (‘dorsomedial’ was defined as an area medial to the greatest curvature of the ventricular roof, presumably corresponding to the location of future primary somatosensory representation; ‘dorsal’ and ‘dorsolateral’ were defined by dividing the remaining pallium into two parts – ‘dorsal’ may correspond to future parietal areas). In vivo data obtained at E13 and those from E14 mice were very similar, probably reflecting that despite the gradient in the initiation of neuronogenesis, the proliferative processes associated with cortical neuronogenesis proceed essentially identically across the lateral to medial axis of the pseudostratified ventricular epithelium (Miyama et al., 1999; Takahashi et al., 1999), and in some parts of the present study they are presented together. Quantification in sections at E15 and older were performed in the dorsal region. For time-lapse recording of DiI-labeled cells in slices, singly and moderately labeled cells were randomly chosen in dorsolateral and dorsal areas in E13 slices and dorsal and dorsomedial areas in E14 slices.

Statistics

In a comparison of two groups (e.g. NS-dividing vs. S-dividing), statistical significance was assessed by chi-square test or Mann-Whitney test. The numbers of samples, as well as the number of cells scored in each sample, are indicated in the figure legends and tables.

Table 1. Assessment of the frequency of P/P divisions

	Age			
	E13	E14	E13+E14	E15
In vivo*				
Ki67-positive/Nissl-positive	90%	83%	87%	56%
Surface divisions in slices†				
Short culture				
Total two-cell clones	15	4	19	6
Ki67-positive:Ki67-positive	11 (73%)	3 (75%)	14 (74%)	2 (33%)
Ki67-positive:Ki67-negative	4 (27%)	1 (25%)	5 (26%)	2 (33%)
Ki67-negative:Ki67-negative	0 (0%)	0 (0%)	0 (0%)	2 (33%)
Extended culture				
Total clones (2~4 cells)			70	
P/P			57 (81%)	
P/N			11 (16%)	
N/N			2 (3%)	

*Fluorescent Nissl stain was used to visualize all cells in the cerebral wall. The proportion of Nissl-positive cells in the VZ and SVZ of the dorsal pallial region (photographed using a 40× objective lens) that were Ki67 positive (Fig. 1B) was calculated (n=546 cells at E13, 612 cells at E14, and 681 cells at E15).

†Daughter cells generated at the ventricular surface were characterized by staining with anti-Ki67 within 4-7 hours from their birth (short culture, Fig. 1C) or by keeping them much longer (extended culture, Fig. 1D,E).

Daughter cells that did not divide beyond the time that many other daughter cells had divided were judged as neurons (N) in the extended culture.

Table 2. Thickness of the cerebral wall at which each P/P-division type was observed

	n	Cerebral wall thickness
P/P total	57	
Type I	13 (23%)	142±5 μm
Type II total	44 (77%)	169±6 μm
Type IIa	23	142±3 μm
Type IIb	21	197±8 μm

Fifty-seven P/P divisions (Table 1) were classified according to the behavior of daughter cells (Figs 1 and 2). All values shown are mean±s.e.m. Differences between type I and type II (P<0.05), type IIa and type IIb (P<0.0001), and type I and IIb (P<0.0001) were significant (Mann-Whitney test), but those between between type I and type IIa were not significant.

Results

P/P divisions predominate during the pre-CP stage

To examine whether P/P divisions are occurring in the VZ of the cerebral wall before the CP appears (Fig. 1A), and if so, how frequently, we used two different approaches (Fig. 1B-E, Table 1). Reactivity with the monoclonal antibody Ki67 (Gerdes et al., 1984) was used as a marker of cycling cells. In frozen sections of freshly prepared cerebral walls (Fig. 1B), the overwhelming majority of VZ and SVZ cells (90% at E13; 84% at E14) were positive for Ki67, but at E15 only 56% stained positive for Ki67. We next immunostained daughter cells generated in slice culture with Ki67 (Fig. 1C,C′). Of the 19 clones generated from a single DiI-labeled progenitor cell at the ventricular surface of E13-E14 slices (4-7 hours after their generation), 74% were composed of two Ki67-positive cells, but only 33% of the clones labeled in E15 slices were such Ki67-positive pairs. We further monitored cellular behavior as an independent means to assess daughter cell type; whether daughter cells born in slices subsequently divide was examined by keeping them for 20 to 30 hours. Of the 70 two-cell clones formed at the ventricular surface of E13-E14 slices, 81% (57 clones) were composed of two mitotic daughters that subsequently divided to form four-cell clones. These results indicate that the P/P division is very common in the pre-CP stage, consistent with previous reports (Chenn and McConnell, 1995; Takahashi et al., 1996b; Cai et al., 2002).

Two patterns of P/P division

The 57 P/P divisions observed in extended slice culture were categorized into two distinct types. Type I: Both daughter cells divided at the ventricular surface (Fig. 1D), designated as $P_{S\text{-}div} \rightarrow P_{S\text{-}div}+P_{S\text{-}div}$. In this type of division, a daughter cell that inherited its parent’s pial process ascended more quickly than its sister cell which extended a new process (Miyata et al., 2001; Miyata et al., 2002), showing a different trajectory of interkinetic nuclear movement as seen in the retinal $P_{S\text{-}div} \rightarrow P_{S\text{-}div}+P_{S\text{-}div}$ clones (Saito et al., 2003). Cell cycle length was similar in these paired mitotic daughters. Type II: One of the mitotic daughter cells divided at a non-surface

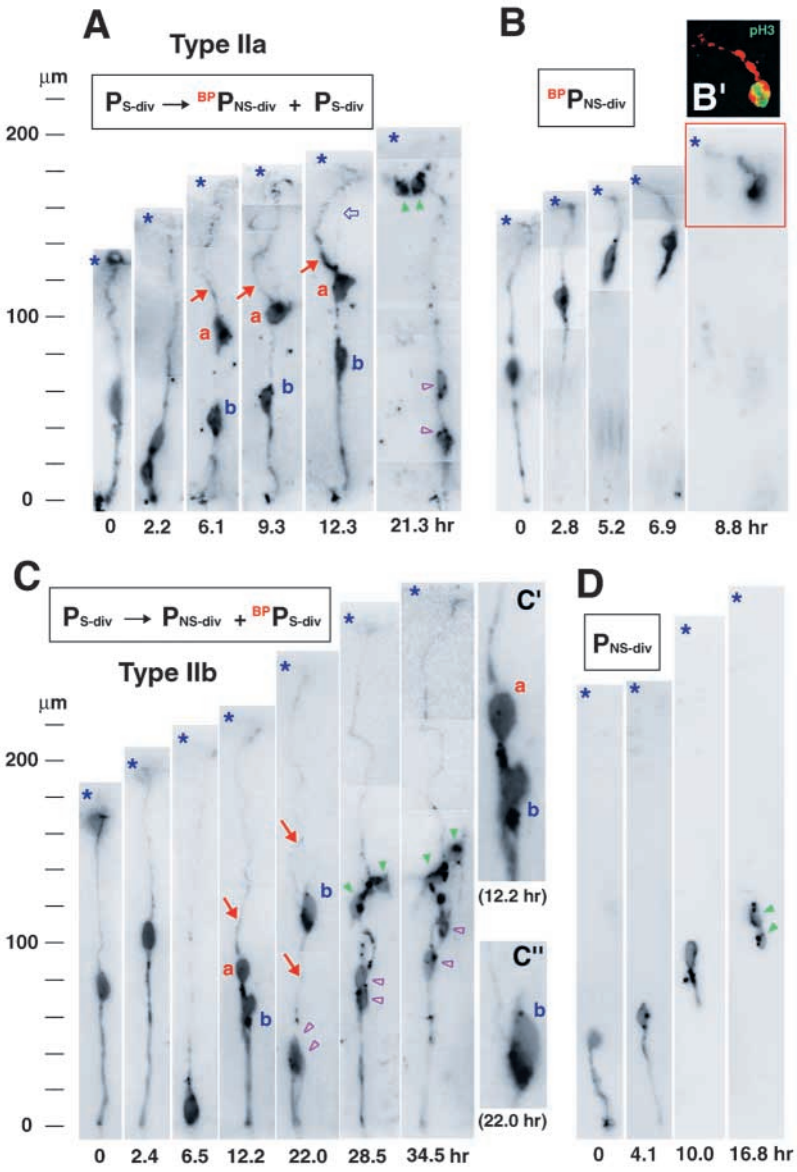

Fig. 2. Two types of NS-dividing cells and two types of $P_{S\text{-}div}$+$P_{NS\text{-}div}$ divisions. (A) Type IIa division gives the parent's basal process (BP) to a NS-dividing daughter cell. Daughter cell 'a' generated in an E13 slice inherited the BP (solid arrow) from the original progenitor cell and divided away from the ventricular surface (designated as $^{BP}P_{NS\text{-}div}$) giving rise to two daughter cells (solid arrowheads). Daughter cell 'b' (designated as $P_{S\text{-}div}$) extended a new radial process (open arrow) to the pial surface and may have divided at the ventricular surface to generate daughter cells in the ventricular zone (VZ) (open arrowheads). (B) A singly DiI-labeled $^{BP}P_{NS\text{-}div}$ cell viewed in greater detail in an E13 slice. Bipolar-to-unipolar transition was evident before NS division (confirmed by pH3 expression, B′). (C) Type IIb division gives the parent's BP to a S-dividing daughter cell. The process-inheriting daughter cell ('a') divided at the ventricular surface ($^{BP}P_{S\text{-}div}$, daughter cells are indicated by open arrowheads), whereas its sister cell ('b') that did not inherit the process (magnified in C′ and C′) divided abventricularly ($P_{NS\text{-}div}$, daughter cells are indicated by solid arrowheads). Of the four granddaughter cells, only one of the daughters generated by 'a' was labeled with BrdU added into culture from 28.5 hours to 34.5 hours (immunostained at 34.5 hours, not shown). See also Fig. 1E for type IIb cellular behaviors. (D) A $P_{NS\text{-}div}$ cell singly labeled with DiI on the ventricular surface underwent ventricular process collapse (4.1 to 10.0 hours).

position, usually in the SVZ and sometimes in the intermediate zone (IZ) (cellular movements that lead to the NS-division will be described later), whereas the other divided at the surface (designated as $P_{S\text{-}div} \rightarrow P_{S\text{-}div}$+$P_{NS\text{-}div}$) (Fig. 1E,E′). Clear differences in cell cycle length were not detected between the daughter cells.

The type II pattern of division was more frequently (44/57, 77%) observed than type I (13/57, 23%). Given the obtained frequencies, 100 P/P divisions at the surface would result in 123 S divisions (23+23+77) and 77 NS divisions, and expected percentage NS-division arising from the P/P surface divisions should be 39% (77/200). However, this figure is greater than the percentage of NS-divisions that we observed by immunostaining with phosphohistone3 (pH3) in vivo (20±1% at E13, *n*=3; 15±1% at E14, *n*=3) as well as values obtained by others (Smart, 1973; Takahashi et al., 1993), and we feel that the division patterns in slice culture are biased from type I divisions towards type II divisions. Anti-pH3 immunostaining on sections made from E13-derived slices revealed time-dependent increase in the percentage of NS divisions: 17±1% at 12 hours (mean±s.e.m., *n*=3); 20±4% at 24 hours (*n*=6); and 31±1% at 36 hours (*n*=8). Nevertheless, the mechanism that facilitates daughter cell choice of an NS or an S division must exist in slices because the majority of daughter cells generated by the 57 cases of P/P division divided at the surface [also notably, all P/N divisions (11 cases) were judged as $P_{S\text{-}div}$+N]. There was a correlation between the frequency of division type and the thickness of the cerebral wall in which the original DiI-labeled progenitor divided (Fig. 1D,E; Table 2; see Fig. S1 at http://dev.biologists.org/supplemental/). The averaged thickness of slices where type II divisions were observed (169±6 µm, mean±s.e.m.) was significantly (P<0.05, Mann-Whitney test) greater than that for type I (142±5 µm).

Origin and morphological changes of NS-dividing daughter cells

We further found that the type II P/P divisions can be classified into two subgroups according to the pattern of the inheritance of the pial process. Type IIa: A daughter cell that inherited its parent's basal process (BP) initially adopted a bipolar morphology, collapsed the ventricular process transforming into a unipolar shape, and finally divided at a NS position just beneath the preplate or immature CP; the other daughter cell extended a new pial process to obtain a bipolar morphology, and descended to divide at the surface ($P_{S\text{-}div} \rightarrow P_{S\text{-}div}$+$^{BP}P_{NS\text{-}div}$) (Fig. 2A,B, also shown later in Fig. 3A, Fig. 4A,B, Fig. 5A, Fig. 6A-C). Type IIb: A daughter cell that did not inherit the parent's pial process initially adopted a marking pin-like morphology,

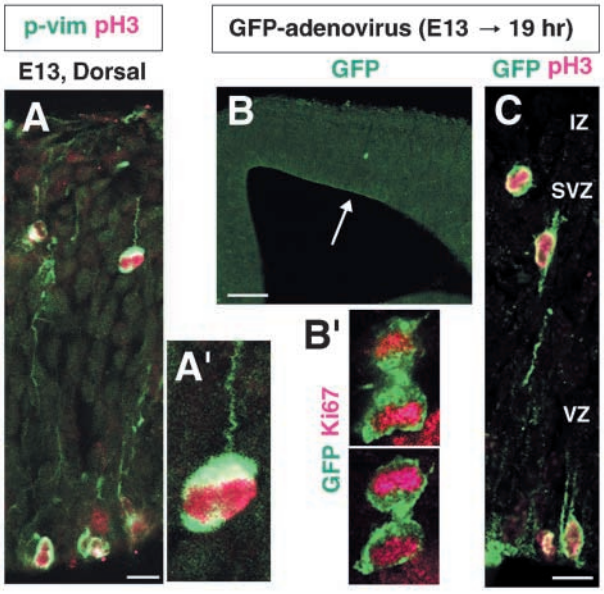

Fig. 3. Morphology and origin of NS-divisions in vivo. (A) Double immunostaining of an E13 cerebral wall section with phosphorylated vimentin (p-vim) and pH3, showing two pia-connected, unipolar-shaped dividing cells (one of them is magnified in A′). (B) A serial section (20 μm thick) from an E14 cerebral hemisphere subjected to GFP-adenovirus injection into the lateral ventricle 19 hours earlier visualized under a fluorescent microscope. Anti-GFP antibody detected only the indicated mitosis (telophase, strongly positive for Ki67; B′) in three serial sections. (C) Visualization of cerebral wall sections from embryos infected with GFP-adenovirus demonstrates GFP^+ cells in both S and NS positions. Scale bars: 10 μm in A,C; 100 μm in B.

ascending its cell body by the extension of a ventricular process ($P_{S\text{-}div} \rightarrow {}^{BP}P_{S\text{-}div}+P_{NS\text{-}div}$) (Fig. 1E, Fig. 2C,D, also shown later in Fig. 3C, Fig. 4C, Fig. 6L-O). After the loss of the ventricular process, it divided in the SVZ or lower half of the IZ. The other daughter cell, which was bipolar-shaped from the beginning of its life, divided at the surface. These two subtypes were observed at similar frequencies [type IIa, 23/57 (40%); type IIb, 21/57 (37%)]. Cycling of the time-lapse recorded cells in slices was a little slower (approximately 15-18 hours in type I and IIa; approximately 20-24 hours in type IIb) compared with that estimated in vivo (11.4 hours at E13 and 15.1 hours at E14) (Takahashi et al., 1995a). Notably, type IIb divisions were observed in significantly ($P<0.0001$, Mann-Whitney test) thicker portions (197±39 μm) compared with type IIa (142±15 μm).

Importantly, each of the NS-dividing cells in slices was born at the ventricular surface and moved to the SVZ within a single cell-cycle length by losing its apical (ventricular) attachment. The collapse of the ventricular process seemed to have started 2-7 hours before M phase and finished 1-5 hours before M phase. Although the ${}^{BP}P_{NS\text{-}div}$ cell (type IIa) after bipolar-to-unipolar change resembles a translocating neuron (Nadarajah et al., 2001), the existence of the unipolar-shaped dividing cells was confirmed in vivo by the use of anti-phosphorylated vimentin (p-vimentin) antibody (Fig. 3A). The p-vimentin antibody also stained isolated NS mitoses in vivo (not shown); these may correspond to the $P_{NS\text{-}div}$ cell of type IIb divisions.

In order to further examine these phenomena in vivo, we injected GFP-adenoviruses into the lateral ventricles of E13 embryos and examined fluorescence 18-19 hours later. As shown in Fig. 3B,C, numerous GFP^+ NS mitoses, along with GFP^+ S mitoses, were observed in the dorsal and dorsolateral regions (in 5 embryos from 3 independent experiments). Because adenovirus infection occurs at the ventricular surface within 4 hours after injection (Hashimoto and Mikoshiba, 2004), the supply of NS-dividing cells from the surface to the SVZ was confirmed. Cell cycle length in the dorsomedial region is reported to be approximately 11.4 hours at E13 (Takahashi et al., 1995a), and it is expected to be longer at the thicker (thus developmentally more advanced) (Smart and McSherry, 1982) regions. Therefore, the detection of the GFP^+ NS-dividing cells at 18-19 hours suggests that the S-to-NS supply of the mitotic daughters in vivo may have occurred within a single cell cycle.

NS mitoses at E13 and E14 are committed to the neuronal lineage and may generate neuron pairs

In the slice culture system, successful immunohistochemical examination of daughter cells generated by NS-dividing cells was possible in 14 cases; these included three type-IIa four-cell clones, five singly labeled ${}^{BP}P_{NS\text{-}div}$ cells, two type-IIb four-cell clones, and four singly labeled $P_{NS\text{-}div}$ cells. Twelve examples were subjected to immunostaining with anti-Hu (16A11) (Marusich et al., 1994); Hu, an RNA-binding protein, has been used as a neuronal marker in the developing cerebral wall (Okano and Darnell, 1997; Miyata et al., 2001). In 11 samples (92%), Hu was detected in both of the NS-derived daughter cells (Fig. 4). Upon division of the ${}^{BP}P_{NS\text{-}div}$ cell, its bp was inherited by one of the Hu^+ daughter cells. Some (though not all) of such process-inherited Hu^+ cells were quickly inserted into the CP (Fig. 4B). In one case (a $P_{NS\text{-}div}$ cell in an E14 slice), both daughter cells were negative for Hu (not shown). One pair of daughter cells from an E14 $P_{NS\text{-}div}$ cell stained with p27, a cell cycle arrest marker (cyclin kinase inhibitor), and both daughter cells were positive (data not shown). One type-IIb clone (case shown in Fig. 2C) was treated with BrdU for 6 hours before fixation and stained for BrdU; only one granddaughter cell born at the surface was positive, whereas the remaining three granddaughters (including those generated by the NS mitosis) were negative (data not shown). These Hu^+, $p27^+$, or $BrdU^-$ daughter cells showed morphologies (translocating- or locomoting-like multipolar) (Nadarajah et al., 2001; Tamamaki et al., 2001; Tabata and Nakajima, 2003) reported for neurons. During the extended observation of daughter cells generated from ${}^{BP}P_{NS\text{-}div}$ or $P_{NS\text{-}div}$ cells (over 30 hours, without immunostaining; n=6 at E13 and n=8 at E14), only one NS-derived daughter cell divided but all others (13 cells) did not. These results strongly suggest that most of the NS mitoses observed in E13-E14 slices may have generated paired neurons (N/N division).

We next sought to determine whether N/N divisions at the NS position also occur frequently in vivo, but the direct lineage tracing was technically very difficult. We therefore took advantage of the observation that Hu is expressed in the peripheral nervous system in some dividing cells that are committed to the neuronal lineage (Marusich et al., 1994). Frozen sections of E13 and E14 cerebral walls were doubly stained with Hu and pH3 (Fig. 5A). Separate immunostaining

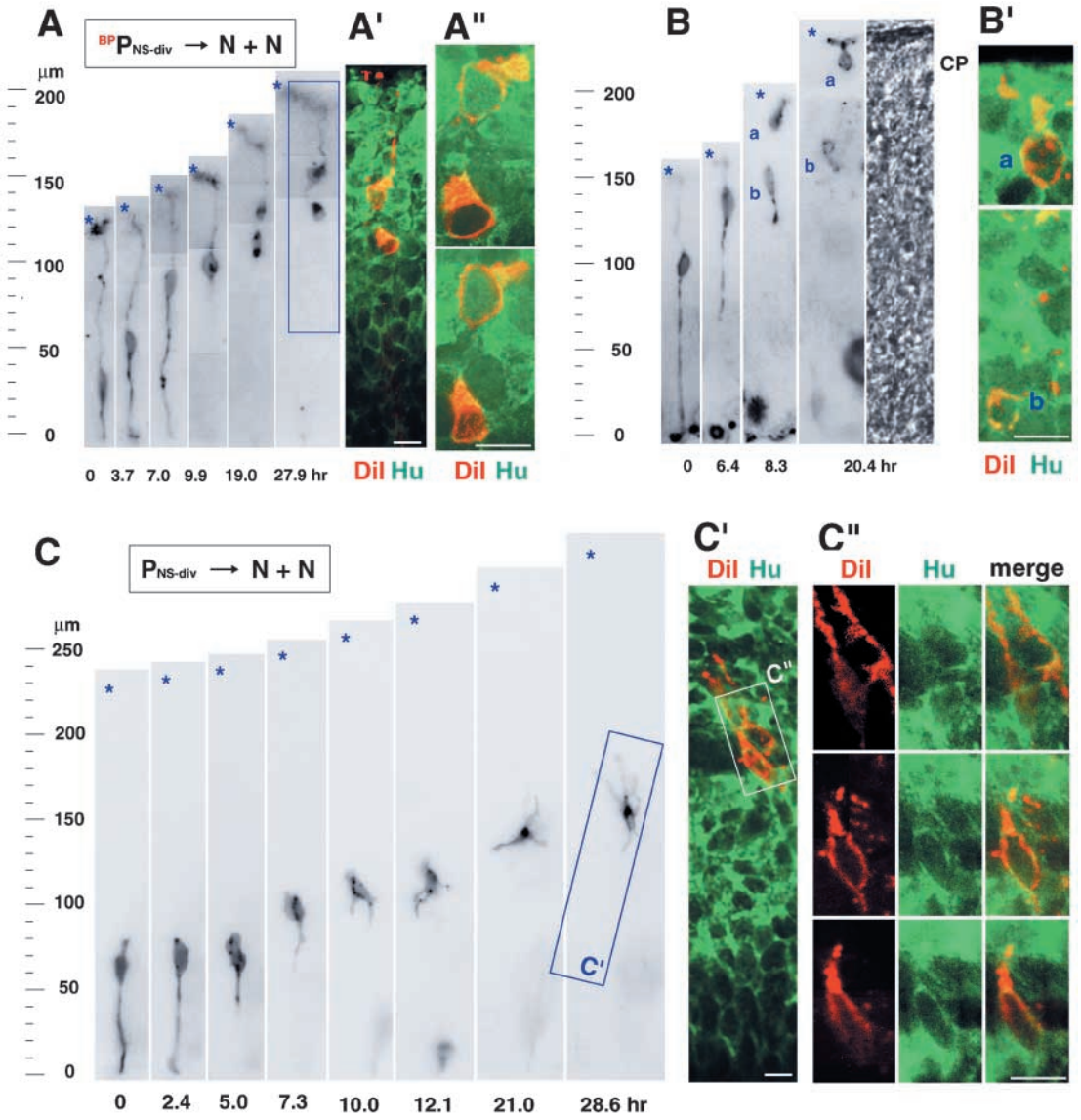

Fig. 4. Immunohistochemical and behavioral characterization of daughter cells generated from NS-dividing cells. (A) A $^{BP}P_{NS\text{-}div}$ cell observed in an E13 slice adopted a unipolar shape and subsequently divided to produce two Hu^+ cells, one of which inherited the pia-connected process. Panels A′ and A′ show merged views of confocal images taken using a 40× (A′) or 100× (A″) objective lens. (B) After undergoing bipolar-to-unipolar change, a $^{BP}P_{NS\text{-}div}$ cell captured in an E13 slice generated two Hu^+ cells (B′, 100×), one of which (cell 'a') ascended more quickly than its sister (cell 'b'), having entered the immature cortical plate (CP) by 20.4 hours. (C) A $P_{NS\text{-}div}$ cell observed in an E14 slice. Division may have occurred by 5.0 hours. Both daughter cells initially had two or three non-radially oriented processes in the subventricular zone (SVZ) (10.0-21.0 hours) and later became more radially oriented and Hu^+ [C′, 40×; C″, photographed at three different planes (100×)] in the lower intermediate zone (28.6 hours), resembling locomotion neurons (Nadarajah et al., 2001). Scale bars: 10 μm in A′,A′,B′,C′,C′.

revealed that NS-dividing cells at E13 and E14 were mostly (85-95%) $Nestin^+$ and were rarely stained with an endothelial cell marker (5-6%). Remarkably, most of the $pH3^+$ NS mitoses (93% at E13; 81% at E14) were Hu^+, whereas the S mitoses were completely negative (Fig. 5B). The Hu^+ index for NS mitoses at E14 was significantly higher ($P<0.0001$, chi-square test) than those obtained for NS mitoses in sections at E17 (38%) and P0 (22%) when gliogenesis predominates over neuronogenesis (LeVine and Goldman, 1988). These results indicate that nearly all of the NS-dividing cells that posses $Nestin^+$ neuroepithelial-like character at E13 and E14 were committed to the neuronal lineage.

Cell cycle-dependent and lineage-restricted expression of Ngn2

In order to identify the molecular mechanisms that allow a mitotic daughter cell to undergo NS division, we focused on Ngn2, a bHLH transcription factor known to be important for commitment to the neuronal lineage (Sommer et al., 1996; Fode et al., 2000; Nieto et al., 2001) (reviewed by Ross et al., 2003). We first compared the expression of Ngn2 protein between S and NS mitoses by using antibodies against Ngn2 (Mizuguchi et al., 2001) and p-vimentin (Fig. 6A-D, Table 3). Ngn2 was sporadically detected in the VZ and SVZ with varying intensity (Fig. 6A), but Nestin, RC2 and Pax6 were all

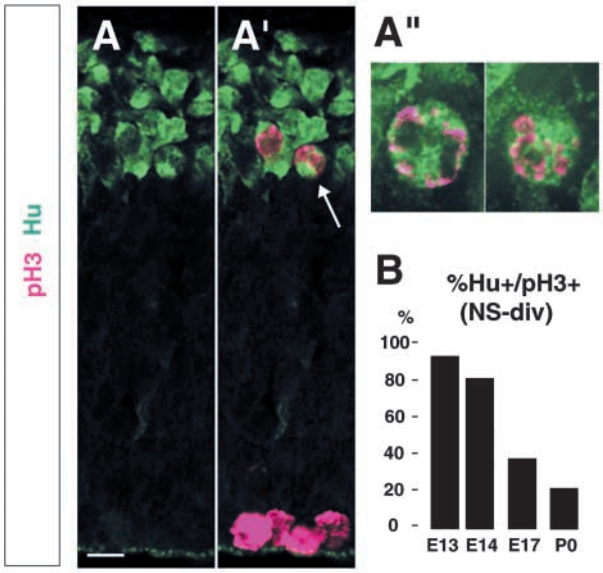

Fig. 5. NS-dividing cells in E13-E14 cerebral walls are mostly Hu$^+$. (A-A″) Hu and pH3 double staining allows for the identification of cells undergoing division in E13 cerebral wall section. Two NS mitoses were clearly Hu$^+$ (A″ shows magnified images of arrowed cell, two different confocal planes at 100×). S-dividing cells (A′) were completely negative for Hu. (B) Quantification of the stage-dependent changes in the proportion of the pH3$^+$ NS-dividing cells that were Hu$^+$ demonstrates decreased anti-Hu reactivity with development (n=332 cells at E13, 267 cells at E14, 221 cells at E17, and 246 cells at P0). Scale bar: 10 μm.

diffusely positive throughout the same area (not shown). The proportion of Ngn2-positive cells out of the total p-vimentin$^+$ cells (mitoses) at the NS position (32%) was significantly (P<0.0001, chi-square test) greater than that observed for the S mitoses (4%).

To explain how this striking difference between NS-dividing and S-dividing cells was generated by M phase and why Ngn2 immunoreactivity was sporadic and non-diffuse, we next used anti-Ki67 antibody (Fig. 6E-K, Table 4). Ki67 expression is graded in a cell cycle-dependent manner: (i) +++, strongest and most diffuse in the largest and round cell bodies in M phase (Fig. 6F,H) [separate double staining with anti-pH3 revealed an absolute correlation of the +++ cells with pH3$^+$ cells (not shown)]; (ii) ++, weaker staining but still very intense in large and triangular cells, these may represent cells around G2 phase (Fig. 6F,H); (iii) +, readily detectable in a punctate pattern by

Table 3. Proportion of Ngn2-positive cells out of the total surface mitoses or non-surface mitoses

	Surface division	Non-surface division
Ngn2-positive/p-vim-positive	4%	32%
Ngn2-positive/Ki67 (+++)	5%	44%

Sections collected from six embryos at E13 or E14 were examined using a confocal microscope (40× or 100× objective).

Total number of p-vim-positive cells counted: 406 cells for S division, 234 cells for NS division.

Total number of Ki67+++ cells counted: 205 cells for S division, 143 cells for NS division.

Differences between the S and NS groups were significant (P<0.0001, chi-square test) in both detection methods.

Table 4. Proportions of Ngn2-positive cells out of the total cycling cells and the cells in particular cell cycle phases

Ngn2 and Ki67	
Total Ki67-positive cells	1623
Ngn2-positive/Ki67-positive	28%
Ngn2-positive/Ki67+++	7%
Ngn2-positive/Ki67++	21%
Ngn2-positive/Ki67+	32%
Total Ngn2-positive cells	575
Ki67-positive/Ngn2-positive	78%
Ngn2 and BrdU	
Total BrdU-positive cells	555
Ngn2-positive/BrdU-positive	21%
Total Ngn2-positive cells	288
BrdU-positive/Ngn2-positive	42%

Sections collected from eight E13 or E14 embryos were examined for Ngn2 and Ki67 colocalization using a confocal microscope (40× objective), and sections from five embryos were similarly examined for Ngn2 and BrdU colocalization. Results were for assessment of cell cycle phases, Ki67 immunoreactivity was graded as presented in Fig. 6F. Ngn2 immunoreactivity was not graded [taking all of the +++ to + (Fig. 6E,G,I) as 'positive'] here.

standard immunostaining protocol (Fig. 6F, see also Fig. 1B,C) but a decreased antibody concentration gave background-like staining (Fig. 6H), which may represent cycling cells in the remaining (G1 and S) phases. We also divided Ngn2-positive cells into three subgroups according to their reactivity [most intense '+++', moderate '++', and weakest '+' (Fig. 6E)]. The proportion of the total Ki67-positive (+++~+) cells that expressed Ngn2 at any level was 28%, whereas the proportion of the total Ngn2-positive (+++~+) cells that expressed Ki67 at any level was 79% (Table 3), indicating that only a portion of the total cycling cell population expresses Ngn2, and Ngn2 is expressed primarily in the cycling population but also in some neurons.

Interestingly, the frequency of observation of Ngn2-positive cells inversely related to Ki67 staining intensity: 32% in Ki67$^+$; 21% in Ki67^{++}; and 7% in Ki67^{+++} (Table 4). In separate quantification, the proportion of S-phase cells (labeled with BrdU, survival time=30 minutes) that were positive for Ngn2 (not shown) was 21% (Table 3). Comparison of percentage Ngn2-positive between the S mitoses and NS mitoses (Ki67^{+++} cells) revealed, as assessed by p-vimentin staining, that Ngn2 expression was significantly (P<0.0001, chi-square test) more frequent in the NS mitoses (44%) than in S mitoses (5%) (Table 2). In Fig. 6G, the relationship between the intensity of Ki67 and that of Ngn2 is fully presented, showing the proportions of the total Ngn2 and Ki67 double positive cells that were scored for any of the 3×3 fractions. Ngn2^{+++} cells were almost limited to the Ki67$^+$ fraction; these cells represent cells early in the cell cycle.

We used slice culture to further examine the relationship between Ngn2 expression and cell cycle progression. Ngn2 immunostaining of DiI-labeled daughter cells within 4-8 hours of their generation (n=7) revealed that some daughter cells were Ngn2^{+++} but others were Ngn2$^+$ or negative (Fig. 6L,M). In addition, moderate Ngn2 immunoreactivity was detected in the marking pin-like cells (Fig. 6N,O, n=3/3) and pia-connected, bipolar-shaped cells (not shown, n=2/2) that were about to lose their ventricular attachment, a critical step preceding or during G2 phase in cells undergoing NS-division (Figs 2-4). In contrast, Ngn2 immunoreactivity was not

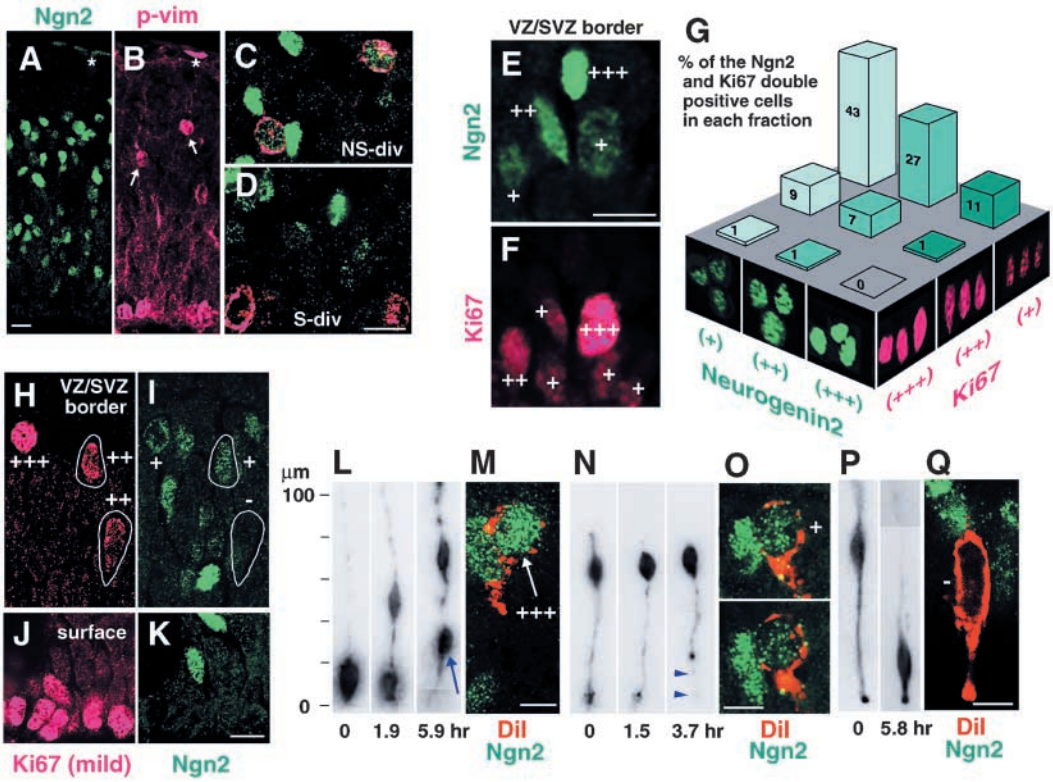

Fig. 6. Ngn2 is expressed in a subset of cycling cells. (A,B) Ngn2 and phosphorylated vimentin (p-vim) double staining at E13 to compare percentage Ngn2$^+$ between S- and NS-dividing cells. Two NS mitoses (arrows in B, merged image photographed with a 100× lens is shown in C) were weakly positive for Ngn2, whereas S mitoses in this field were all Ngn2-negative (some are magnified in D). See Table 3 for quantification. Pial surface is indicated with asterisk. (E,F) Ngn2 and Ki67 double staining to examine Ngn2 expression in relation to cell cycling. Our grading of Ngn2 and Ki67 intensity is exemplified using a picture taken at the ventricular zone (VZ)/subventricular zone (SV) border of an E14 section. The presented 7 cells included a Ngn2^{+++}Ki67$^-$ cell, a Ngn2^{++}Ki67$^+$ cell, a Ngn2$^+$Ki67^{+++} cell, a Ngn2$^+$Ki67^{++} cell, and three Ngn2$^-$Ki67$^+$ cells. In separate staining of equivalent sections, Ki67^{+++} cells were nearly always pH3$^+$ (not shown). (G) There was an observed relationship between the intensity of Ki67 immunoreactivity and that of Ngn2 immunoreactivity. Graph shows the proportion of cells in each of the 3×3 fractions (0~43%) out of the total cells that were simultaneously positive (+~+++) for Ki67 and Ngn2 (100%); indicated values are obtained from 458 cells examined using a confocal microscope (see also Table 4). (H-K) Milder treatment with anti-Ki67 visualizes cells during or just prior to division. By using diluted anti-Ki67 antibody (5-10 times lower in concentration compared with one used for Fig. 1B,C, Fig. 6F,G), Ki67^{+++} or Ki67^{++} cells were more clearly discriminated from Ki67$^+$ cells which were only faintly visualized. Under these conditions, the proportion of Ngn2-positive cells out of the Ki67^{+++} cells was obtained for either of the S-dividing and NS-dividing populations (Table 3). In this field, one NS-dividing cell was Ngn2$^+$, but S-dividing cells were all Ngn2$^-$. Of the two Ki67^{++} cells (outlined), the upper cell was Ngn2$^+$, whereas the lower, triangular-shaped cell was Ngn2$^-$. (L-Q) Anti-Ngn2 staining on time-lapse monitored cells to examine cell cycle-dependent and lineage-restricted expression of Ngn2. Strongest immunoreactivity was observed in some (but not all) of the cells 4-8 hours after generation [L,M: the indicated daughter cell was Ngn2^{+++}, whereas the other was Ngn2$^-$ (not shown); cerebral wall thickness at 0 hour was approximately 180 μm]. (N,O) Pin-like cells losing the ventricular process (arrowheads in N) showed a moderate level of Ngn2 expression (O, photographed at two different planes). (P,Q) We could not detect Ngn2 expression in cells quickly moving towards the ventricular surface. Scale bars: 10 μm in A-F,H-K,M,O,Q.

detected in DiI-labeled cells that were captured during their G2-like movement towards the ventricular surface (n=21) (Fig. 6P,Q). These data obtained through combined approaches indicate that Ngn2 expression is limited to a certain cycling population from as early as G1 phase and further restricted in a lineage-dependent fashion consistent with a bias towards the NS-dividing population, and that Ngn2 expression in cycling cells is strongest in G1 phase and subsequently declines.

Conversion of S division to NS division by Ngn2 retrovirus

The above results prompted us to hypothesize that Ngn2 might be involved in the morphological changes that cause a cycling daughter cell to lose its ventricular attachment and migrate to the SVZ or IZ for NS division. To test this possibility, we injected a retrovirus containing ngn2 and GFP genes, along with injecting a control GFP virus, into lateral ventricles of mouse embryos (Fig. 7A). Considering the delayed onset of expression of introduced genes, injections were made at E12 and examinations to identify the position of GFP and pH3 double positive cells were mostly performed 48 hours later (E14) (Fig. 7B-I). In the control treated group (7 embryos from 3 independent experiments), the majority of GFP$^+$ dividing cells (45 cells per embryo on average) were found at the ventricular surface (Fig. 7B-D), providing a percentage NS-division of 26±3% (mean±s.e.m.) (Fig. 7I). In contrast, embryos injected with Ngn2 virus (n=9 from 3 independent experiments) showed a reversed S:NS ratio (Fig. 7E-I). The proportion of GFP$^+$ dividing cells (10 cells per embryo on average) that were found at the NS position (73±3%) was significantly higher (P<0.001, Mann-Whitney test) than that seen in control treated samples. We confirmed the expression of Ngn2 in GFP$^+$ NS dividing cells (2/2) (Fig. 7H), although all cells were not stained to determine precise Ngn2 expression rates. A similar predominance of NS divisions was detected at 24 hours (n=3, 75-90%) and 36 hours (n=4, 75-85%) after injection of Ngn2 virus at E12. These results, together with the spatiotemporal pattern of Ngn2 expression (Fig. 6), strongly

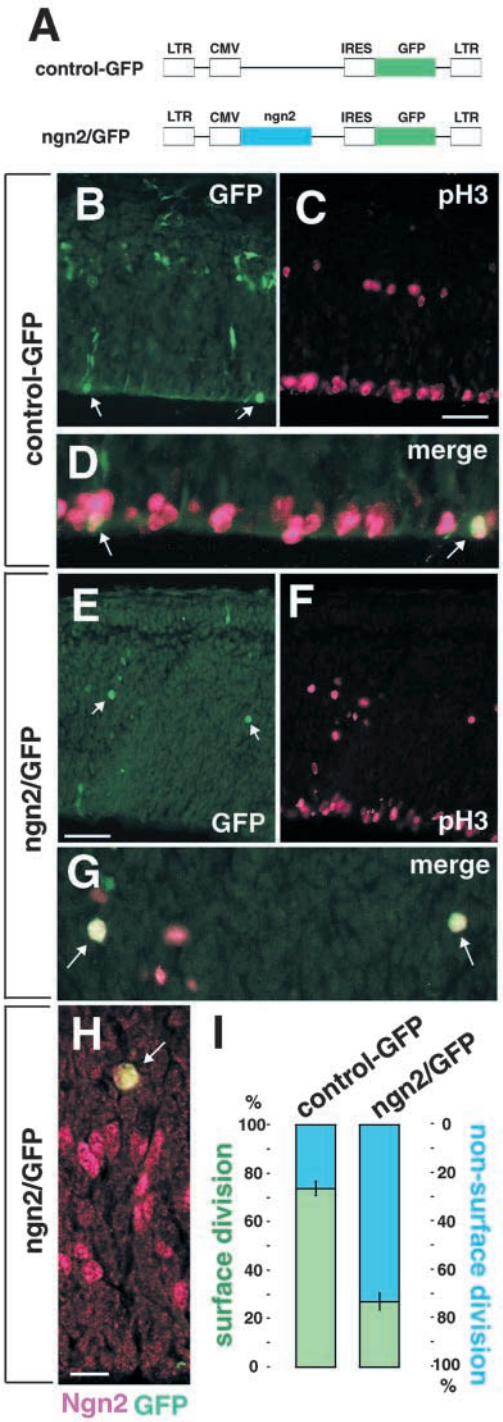

Fig. 7. NS-divisions induced by retrovirus-mediated Ngn2 expression. (A) Retroviral vectors used in this study. (B-D) Section of an E14 cerebral wall infected with the control-GFP virus 48 hours earlier, doubly stained with anti-GFP and anti-pH3 showing two GFP^+ mitoses at the ventricular surface (arrows). (E-G) Section of an E14 cerebral wall infected with the ngn2/GFP virus 48 hours earlier showing two GFP^+ mitoses in the NS position (arrows). (H) Retroviral infection leads to expression of Ngn2 by a GFP^+ mitosis at the NS position of a ngn2-introduced cerebral wall. (I) NS mitoses are significantly increased ($P<0.001$ compared with control) in ngn2 retrovirus-treated samples ($n=7$ for control-GFP, $n=9$ for ngn2/GFP; mean±s.e.m.). Scale bars: 10 μm in B,C,E,F,H. CMV, cytomegalovirus promoter; IRES, internal ribosomal entry site; GFP, green fluorescent protein; LTR, long terminal repeat.

suggest that Ngn2 is involved in the choice of mitosis position during E13-E14.

Discussion

NS mitoses in the pre-CP stage favor N/N division

The present study strongly supports the hypothesis that NS mitoses produce CP neurons (Smart, 1973). We directly observed that E13-14 mitoses in the SVZ or lower IZ produced pairs of daughter cells that showed immunoreactivity (Hu or p27), morphologies (translocating- or locomoting-like; multipolar) (Nadarajah et al., 2001; Tamamaki et al., 2001; Tabata and Nakajima, 2003), and movements typical of young neurons (Fig. 4). Therefore, we believe that these NS divisions produced pairs of neurons in slice culture.

In vivo, Hu immunoreactivity in almost all the $Nestin^+$ mitoses indicated the complete commitment of this secondary mitotic population to the neuronal lineage during E13-E14 (Fig. 5). This means, however, that detection of Hu alone cannot be considered as proof in identifying a cell as a neuron; one extreme interpretation of our observation that NS mitoses produced paired Hu^+ cells in slices would be that many of the Hu^+ NS-derived daughter cells were neuronal progenitor. Nevertheless, we still consider that the most likely mitosis pattern taken by these NS-dividing cells in vivo must be $P_{NS\text{-}div} \rightarrow N+N$.

The number of NS mitoses is limited to 10-20% of the total mitoses during this stage, this means that only a few, if any, of the NS-derived Hu^+ daughter cells as observed in slices can divide in vivo. A previous study by Takahashi and colleague (Takahashi et al., 1995b) reported an increase in the relative size of the 'secondary proliferative population', which corresponds to the NS-dividing population, during E14-E15 (approximately 2.4 times expansion) and concluded that only 14% of the NS-derived daughter cells could be neurons (thus the division pattern should primarily be non-terminal). This study did not take into account the possibility that mitotic cells are continuously supplied from the ventricular surface to the NS position (to allow most of the preexisting NS cells to undergo terminal N/N divisions while allowing the overall NS-dividing population to expand); we demonstrated that this is, in fact, the case at E14 (Figs 1-3, Table 4). These lines of evidence suggest that most Hu^+ daughter cells that would be generated from Hu^+ NS mitoses in vivo may not subsequently divide. In addition, the frequency of N/N division at the ventricular surface (i.e. production of two daughter cells that did not divide beyond the time that many other daughter cells had divided to form 3- or 4-cell clones) was low (3%, Table 1) in the present study. This rate would not sufficiently explain the existence of N/N divisions during early corticogenesis in vivo that has been evidenced in mice (Cai et al., 2002) and suggested in rats (Noctor et al., 2001). We must therefore conclude that the mode of division most heavily favored by the in vivo NS mitoses during the pre-CP stage is N/N (Fig. 8A).

NS mitoses as the major source of the deep CP neurons

The idea of N/N-dominant divisions by $P_{NS\text{-}div}$ cells can be used

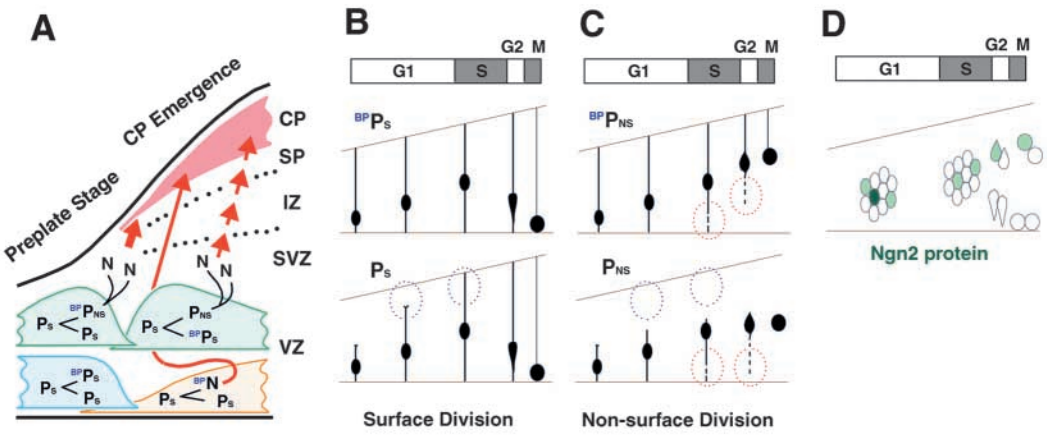

Fig. 8. Asymmetric P/P division for preparation of efficient neuron release. (A) Schematic illustration showing division patterns that we observed in the pre-cortical plate (CP) stage. SP, subplate. (B,C) Morphological changes observed in S-dividing (B) and NS-dividing (C) cells during the progression of their cell cycle. In the upper panels, mitotic daughter cells that inherited the basal process ($^{BP}P_{S\text{-}div}$ and $^{BP}P_{NS\text{-}div}$) are shown; the lower panels depict non-inheritors ($P_{S\text{-}div}$ and $P_{NS\text{-}div}$). (D) Ngn2 expression is lineage restricted and varies with the cell cycle.

to estimate the degree of contribution of NS mitoses to the total output of early CP neurons, with the help of Takahashi and colleague (Takahashi et al., 1996b) who performed rigid quantification on the proportions of daughter cells that exit the cell cycle ('Q fraction') or not ('P fraction') from the overall mitotic population (not the S-dividing or NS-dividing populations alone) at E13 and E14. Provided 100 daughter cells are to be generated from 50 divisions, the number of neurons ('Q') generated from the overall mitotic population is expected to be 19 at E13 and 34 at E14 (Takahashi et al., 1996b). Alternatively, the number of NS mitoses is approximately 10 (out of 50 divisions) at E13 (Smart, 1973) (present study); it ranges from approximately 5.5 (Takahashi et al., 1993) to approximately 7.5 (present study) at E14. By multiplying these numbers for the NS division (10 and 5.5-7.5 mitoses at the SVZ) by 2 (for the most extreme example of N/N dominance), the numbers of neurons generated from the NS-dividing population at E13 and E14 obtained are 20 and 11-15, respectively, showing the contribution of NS-derived neurons to the total neuronal output as almost 100% (20/19) and 32-44% (11/34-15/34), respectively. Although the division pattern of the NS mitoses needs to be examined further, we agree with Smart (Smart, 1973) in that the NS-dividing cells are the most important source of E13-generated CP neurons [which correspond to the majority of the deep (layer VI and V) CP neurons] (Caviness, 1982; Takahashi et al., 1999).

Because the E13-born CP neurons are the first to split the preexisiting preplate, we were curious as to how they behave in *reeler* mice which do not show such splitting (Caviness, 1982). Our pH3 immunostaining of frozen sections and use of slice culture to monitor single cells revealed that NS-directed progenitors at E13 ($^{BP}P_{NS\text{-}div}$ cells) are normal in both their mitosis position and preceding morphological changes (nuclear movements and bipolar-to-unipolar change as shown in Figs 2, 4) (T. Miyata, unpublished).

Asymmetric P/P division for efficient neuron/progenitor segregation

The most effective means to expand the mitotic population is through paired daughter cells generated from a progenitor cell individually giving rise to paired mitotic daughters (P→2P→4P). The type I P/P division that we observed in the pre-CP stage (Fig. 1A,D, Table 2) may account for such an expansion of the progenitor pool (Fig. 8A). During the next developmental phase, one can expect some degree of neuron release, for example, production of 2 neurons and 2 mitotic daughters (2N+2P) after two rounds of cell cycling, which could be obtained by asymmetric division at either of the first or second rounds of division: two N/P divisions after symmetric P/P division [P→P (→N/P) + P (→N/P), model 1] or asymmetric P/P division followed by N/N and P/P division [P→P (→N/N) +P (→P/P), model 2]. From our observation of the type II P/P divisions (Fig. 1E, Fig. 2A,C, Table 2), it is suggested that the cerebral wall at E13, just before the emergence of the CP, favors the latter, often launching one mitotic daughter to the SVZ for subsequent production of the earliest CP neurons, with much less frequent N/P divisions (Table 1). Although direct observation has not been possible so far, there may be lineage continuity from type IIa to type IIb, making one mitotic daughter (P_S) generated in a type IIa division behave as a parent cell in type IIb (Fig. 8A). Given the observed mitotic positions, model 1 can be regarded as P_S→P_S (→N/P)+P_S (→N/P) and model 2 as P_S→P_{NS} (→N/N)+P_S (→P/P). The most important difference between these two models is the rate of the segregation of neurons and mitotic cells.

Model 1 requires neurons to evacuate from the ventricular surface to prepare a vacant space for descending G2-phase cells, and it further requires cycling cells to stay in a limited space until new-born neurons exit the VZ, which takes up to 10 hours (Takahashi et al., 1996a). Model 2 does not have these constraints. Considering the high productivity of the VZ during the period of CP emergence (Smart, 1973; Takahashi et al., 1996b), model 1 would not be the best way to avoid cellular congestion (Smart, 1973) in the VZ. Therefore, the asymmetric P/P division that we observed can be considered to be a means for the cerebral wall to combine most efficiently the supply of early CP neurons and the expansion of the cycling cell population. The contribution of NS-divisions to the production of late-born (upper-layer) CP neurons has just been demonstrated most convincingly in the rat (Noctor et al., 2004). It seems appropriate to consider the NS neuronogenic division as a histogenetic tool that has already evolved in the rodent (Smart, 1973; Haubensak et al., 2004) and may have eventually allowed primates to develop unique morphological features,

such as the 'outer subventricular zone' (Smart et al., 2002), rather than taking it as a primate-specific system (Letinic et al., 2002).

Morphological signs of fate commitment during cell cycle progression

Figures 8B,C summarize the changes in the morphology of S- and NS-dividing progenitor cells observed in E13-14 slices. The proportions of individual cell cycle phases indicated at the top are principally based on the findings of Takahashi et al. (Takahashi et al., 1995a). For example, bipolar-to-unipolar changes that are specific to $^{BP}P_{NS\text{-}div}$ cells, observed approximately 2-5 hours before M-phase (Fig. 2B, Fig. 4A,B), are illustrated below S- and G2-phases (Fig. 8C, upper panel) considering time for G2+M (2 hours) and S (approximately 4 hours) in vivo. Similarly, the collapse of a ventricular process in the marking pin-like $P_{NS\text{-}div}$ cells (Fig. 2C, Fig. 4C) is shown during S-G2 phases (Fig. 8C, lower panel). This irreversible transformation prior to a NS-division may always be accompanied by commitment to the neuronal lineage and also in most cases by a decision for a N/N division. Previous transplantation experiments on ferrets (McConnell and Kaznowski, 1991) indicated that commitment of a neuron to take a deep-layer (layer VI) fate occurs in its parent cell late in S-phase or at the S-to-G2 transition. Although we are currently not sure whether our observation can directly explain these results, the detection of irreversible cell fate determination at very similar time points with these two completely different approaches is remarkable.

Another sign for intracellular events that might be accompanied by or linked with fate determination was detected in earlier timing (Fig. 8B,C, lower panels). Whether a daughter cell that does not inherit its parent's bp extends a new process to the pial surface ($P_{S\text{-}div}$) or not ($P_{NS\text{-}div}$) can be distinguished within 10 hours after the cell's birth (Fig. 1B, Fig. 2C), and this choice was suggested to occur in G1 phase (5.5 hours at E13 and 9.3 hours at E14 in vivo) (Takahashi et al., 1995a).

G1 has also been noted as a phase when the strongest and widest Ngn2 expression was detected (Fig. 6); Ngn2 seems to be expressed in a subset (33%, Table 3) of mitotic daughters with varying intensity (Fig. 6G). Its expression is more restricted to fewer cycling cells from S (approximately 23%) through G2 (approximately 20%), along with the disappearance of strongly positive cells. Although the direct measurement of Ngn2 labeling in G2-phase cells destined for NS division was difficult, the probability of Ngn2 expression in cells during or just prior to S divisions, which are roughly four- to eight-times more numerous than NS divisions, was low (3-5%), and therefore the majority of the $Ngn2^+$ G2 cells seem to be determined to divide abventricularly. This spatiotemporal pattern (Fig. 8D) is very comparable with the above mentioned morphological signs that are closely associated with NS divisions. Most likely, mitotic daughter cells infected with Ngn2 virus (Fig. 7) may have taken such morphological changes to take NS positions during their cell cycling. Because P/N divisions that we observed in the present study (11 cases) were all judged as $P_{S\text{-}div} \rightarrow P_{S\text{-}div}+N$ and we found that Ngn2 was expressed in some neurons (Table 3), Ngn2 might also be involved in differential daughter cell movements in P/N divisions, which should be examined in the future. It also remains to be determined regarding the nature of the $Ngn2^+$ S-dividing cells.

At E15 in Ngn2/Mash1 double knock-out mice (Nieto et al., 2001), the position of S-phase cells is abnormally high (scattered throughout the cerebral wall). This could be a paradox between their findings and our demonstration of increased NS divisions by Ngn2 expression. One plausible explanation would be that the extra VZ S-phase cells found in $Ngn2^{-/-}$/$Mash1^{-/-}$ mice may be of the glial lineage (Nieto et al., 2001). Another possibility predicts that Ngn2 might have a negative effect on the elongation of the ventricular process (ascent of the nucleus) late in G1 phase, the absence of which should result in the extra VZ S-phase cells regardless of a role in S-G2 phases for NS-division that we propose. Because Ngn2 is expressed in the mouse retina where no NS divisions are seen, it is likely that the NS-directing effect of Ngn2 may be exhibited in the context of region-specific histogenesis.

We thank Ryoichiro Kageyama, Jacqueline E. Lee and Masato Nakafuku for plasmids and antibodies; Mitsuhiro Hashimoto for instruction on adenovirus work; Kazuhiro Ikenaka for retrovirus packaging cells and instruction; Syu-ichi Hirai, Fumio Matsuzaki, Hideyuki Okano, Noriko Osumi, Shin-ichi Nakagawa and Takashi Takeuchi for helpful discussions.

References

Altman, J. and Bayer, S. A. (1990). Vertical compartmentation and cellular transformations in the germinal matrices of the embryonic rat cerebral cortex. *Exp. Neurol.* **107**, 23-35.

Cai, L., Hayes, N. L., Takahashi, T., Caviness, V. S., Jr and Nowakowski, R. S. (2002). Size distribution of retrovirally marked lineages matches prediction from population measurements of cell cycle behavior. *J. Neurosci. Res.* **69**, 731-744.

Caviness, V. S., Jr (1982). Neocortical histogenesis in normal and reeler mice: a developmental study based upon ^{3}H-thymidine autoradiography. *Dev. Brain Res.* **4**, 293-302.

Chenn, A. and McConnell, S. K. (1995). Cleavage orientation and the asymmetric inheritance of Notch1 immunoreactivity in mammalian neurogenesis. *Cell* **82**, 631-641.

Estivill-Torrus, G., Pearson, H., van Heyningen, V., Price, D. J. and Rashbass, P. (2002). Pax6 is required to regulate the cell cycle and the rate of progression from symmetrical to asymmetrical division in mammalian cortical progenitors. *Development* **129**, 455-466.

Ferguson, K. L., Vanderluit, J. L., Hebert, J. M., McIntosh, W. C., Tibbo, E., MacLaurin, J. G., Park, D. S., Wallace, V. A., Vooijs, M., McConnell, S. K. et al. (2002). Telencephalon-specific Rb knockouts reveal enhanced neurogenesis, survival and abnormal cortical development. *EMBO J.* **21**, 3337-3346.

Fishell, G. and Kriegstein, A. R. (2003). Neurons from radial glia: the consequences of asymmetric inheritance. *Curr. Opin. Neurobiol.* **13**, 34-41.

Fode, C., Ma, Q., Casarosa, S., Ang, S. L., Anderson, D. J. and Guillemot, F. (2000). A role for neural determination genes in specifying the dorsoventral identity of telencephalic neurons. *Genes Dev.* **14**, 67-80.

Gerdes, J., Lemke, H., Baisch, H., Wacker, H. H., Schwab, U. and Stein, H. (1984). Cell cycle analysis of a cell proliferation-associated human nuclear antigen defined by the monoclonal antibody Ki-67. *J. Immunol.* **133**, 1710-1715.

Hashimoto, M. and Mikoshiba, K. (2004). Neuronal birth date-specific gene transfer with adenoviral vectors. *J. Neurosci.* **24**, 286-296.

Haubensak, W., Attardo, A., Denk, W. and Huttner, W. B. (2004). Neurons arise in the basal neuroepithelium of the early mammalian telencephalon: a major site of neurogenesis. *Proc. Natl. Acad. Sci. USA* **101**, 3196-3201.

He, W., Ingraham, C., Rising, L., Goderie, S. and Temple, S. (2001). Multipotent stem cells from the mouse basal forebrain contribute GABAergic neurons and oligodendrocytes to the cerebral cortex during embryogenesis. *J. Neurosci.* **21**, 8854-8862.

Ishii, Y., Nakamura, S. and Osumi, N. (2000). Demarcation of early

mammalian cortical development by differential expression of fringe genes. *Dev. Brain Res.* **119**, 307-320.

Knoblich, J. (2001). Asymmetric cell division during animal development. *Nat. Rev. Mol. Cell. Biol.* **2**, 11-20.

Letinic, K., Zoncu, R. and Rakic, P. (2002). Origin of GABAergic neurons in the human neocortex. *Nature* **417**, 645-649.

LeVine, S. M. and Goldman, J. E. (1988). Embryonic divergence of oligodendrocyte and astrocyte lineages in developing rat cerebrum. *J. Neurosci.* **8**, 3992-4006.

Marusich, M. F., Furneaux, H. M., Henion, P. D. and Weston, J. A. (1994). Hu neuronal proteins are expressed in proliferating neurogenic cells. *J. Neurobiol.* **25**, 143-155.

McLean, I. W. and Nakane, P. K. (1974). Periodate-lysine-paraformaldehyde fixative. A new fixation for immunoelectron microscopy. *J. Histochem. Cytochem.* **22**, 1077-1083.

Miyama, S., Takahashi, T., Nowakowski, R. S. and Caviness, V. S., Jr (1999). A gradient in the duration of the G1 phase in the murine neocortical proliferative epithelium. *Cereb. Cortex* **7**, 678-689.

Miyata, T., Kawaguchi, A., Okano, H. and Ogawa, M. (2001). Asymmetric inheritance of radial glial fibers by cortical neurons. *Neuron* **31**, 727-741.

Miyata, T., Kawaguchi, A., Saito, K., Kuramochi, H. and Ogawa, M. (2002). Visualization of cell cycling by an improvement in slice culture methods. *J. Neurosci. Res.* **69**, 861-868.

Mizuguchi, R., Sugimori, M., Takebayashi, H., Kosako, H., Nagao, M., Yoshida, S., Nabeshima, Y., Shimamura, K. and Nakafuku, M. (2001). Combinatorial roles of olig2 and neurogenin2 in the coordinated induction of pan-neuronal and subtype-specific properties of motoneurons. *Neuron* **31**, 757-771.

Nadarajah, B., Brunstrom, J. E., Grutzendler, J., Wong, R. O. and Pearlman, A. L. (2001). Two modes of radial migration in early development of the cerebral cortex. *Nat. Neurosci.* **4**, 143-150.

Nanmoku, K., Kawano, M., Iwasaki, Y. and Ikenaka, K. (2003). Highly efficient gene transduction into the brain using high-titer retroviral vectors. *Dev. Neurosci.* **25**, 152-161.

Nieto, M., Schuurmans, C., Britz, O. and Guillemot, F. (2001). Neural bHLH genes control the neuronal versus glial fate decision in cortical progenitors. *Neuron* **29**, 401-413.

Noctor, S. C., Flint, A. C., Weissman, T. A., Dammerman, R. S. and Kriegstein, A. R. (2001). Neurons derived from radial glial cells establish radial units in neocortex. *Nature* **409**, 714-720.

Noctor, S. C., Martinez-Cerdeno, V., Ivic, L. and Kriegstein, A. R. (2004). Cortical neurons arise in symmetric and asymmetric division zones and migrate through specific phases. *Nat. Neurosci.* **7**, 136-144.

Nowakowski, R. S., Caviness, V. S., Jr, Takahashi, T. and Hayes, N. L. (2002). Population dynamics during cell proliferation and neuronogenesis in the developing murine neocortex. *Results Probl. Cell Differ.* **39**, 1-25.

Okano, H. J. and Darnell, R. B. (1997). A hierarchy of Hu RNA binding proteins in developing and adult neurons. *J. Neurosci.* **17**, 3024-3037.

Qian, X., Goderie, S. K., Shen, Q., Stern, J. H. and Temple, S. (1998). Intrinsic programs of patterned cell lineages in isolated vertebrate CNS ventricular zone cells. *Development* **125**, 3143-3152.

Ross, S. E., Greenberg, M. E. and Stiles, C. D. (2003). Basic helix-loop-helix factors in cortical development. *Neuron* **39**, 13-25.

Saito, K., Kawaguchi, A., Kashiwagi, S., Yasugi, S., Ogawa, M. and Miyata, T. (2003). Morphological asymmetry in dividing retinal progenitor cells. *Dev. Growth Differ.* **45**, 219-229.

Smart, I. H. (1973). Proliferative characteristics of the ependymal layer during the early development of the mouse neocortex: a pilot study based on recording the number, location and plane of cleavage of mitotic figures. *J. Anat.* **116**, 67-91.

Smart, I. H. and McSherry, G. M. (1982). Growth patterns in the lateral wall of the mouse telencephalon. II. Histological changes during and subsequent to the period of isocortical neuron production. *J. Anat.* **134**, 415-442.

Smart, I. H., Dehay, C., Giroud, P., Berland, M. and Kennedy, H. (2002). Unique morphological features of the proliferative zones and postmitotic compartments of the neural epithelium giving rise to striate and extrastriate cortex in the monkey. *Cereb. Cortex* **12**, 37-53.

Sommer, L., Ma, Q. and Anderson, D. J. (1996). Neurogenins, a novel family of atonal-related bHLH transcription factors, are putative mammalian neuronal determination genes that reveal progenitor cell heterogeneity in the developing CNS and PNS. *Mol. Cell. Neurosci.* **8**, 221-241.

Tabata, H. and Nakajima, K. (2003). Multipolar migration: the third mode of radial neuronal migration in the developing cerebral cortex. *J. Neurosci.* **23**, 9996-10001.

Takahashi, T., Nowakowski, R. S. and Caviness, V. S., Jr (1993). Cell cycle parameters and patterns of nuclear movement in the neocortical proliferative zone of the fetal mouse. *J. Neurosci.* **13**, 820-833.

Takahashi, T., Nowakowski, R. S. and Caviness, V. S., Jr (1995a). The cell cycle of the pseudostratified ventricular epithelium of the embryonic murine cerebral wall. *J. Neurosci.* **15**, 6046-6057.

Takahashi, T., Nowakowski, R. S. and Caviness, V. S., Jr (1995b). Early ontogeny of the secondary proliferative population of the embryonic murine cerebral wall. *J. Neurosci.* **15**, 6058-6068.

Takahashi, T., Nowakowski, R. S. and Caviness, V. S., Jr (1996a). Interkinetic and migratory behavior of a cohort of neocortical neurons arising in the early embryonic murine cerebral wall. *J. Neurosci.* **16**, 5762-5776.

Takahashi, T., Nowakowski, R. S. and Caviness, V. S., Jr (1996b). The leaving or Q fraction of the murine cerebral proliferative epithelium: a general model of neocortical neuronogenesis. *J. Neurosci.* **16**, 6183-6196.

Takahashi, T., Nowakowski, R. S. and Caviness, V. S., Jr (1999). Sequence of neuron origin and neocortical laminar fate: relation to cell cycle of origin in the developing murine cerebral wall. *J. Neurosci.* **19**, 10357-10371.

Tamamaki, N., Nakamura, K., Okamoto, K. and Kaneko, T. (2001). Radial glia is a progenitor of neocortical neurons in the developing cerebral cortex. *Neurosci. Res.* **41**, 51-60.

Tarabykin, V., Stoykova, A., Usman, N. and Gruss, P. (2001). Cortical upper layer neurons derive from the subventricular zone as indicated by Svet1 gene expression. *Development* **128**, 1983-1993.

Valverde, F., De Carlos, J. A. and Lopez-Mascaraque, L. (1995). Time of origin and early fate of preplate cells in the cerebral cortex of the rat. *Cereb. Cortex* **5**, 483-493.

Yoshimatsu, T., Tamura, M., Kuriyama, S. and Ikenaka, K. (1998). Improvement of retroviral packaging cell lines by introducing the polyomavirus early region. *Hum. Gene Ther.* **9**, 161-172.